ACS APPLIED MATERIALS & INTERFACES

www.acsami.org

Research Article

Efficient Removal of Cs^+ and Sr^{2+} Ions by Granulous $(Me_2NH_2)_{4/3}(Me_3NH)_{2/3}Sn_3S_7{\cdot}1.25H_2O$/Polyacrylonitrile Composite

Jilong Li, Jiance Jin, Yanmin Zou, Haiyan Sun, Xi Zeng, Xiaoying Huang, Meiling Feng,* and Mercouri G. Kanatzidis*

Cite This: *ACS Appl. Mater. Interfaces* 2021, 13, 13434−13442

Read Online

ACCESS | Metrics & More | Article Recommendations | Supporting Information

ABSTRACT: The need to effectively and selectively remove radioactive ^{137}Cs and ^{90}Sr from nuclear waste solutions persists to mitigate their environmental mobility and high radiotoxicity. Because it is difficult to effectively remove them from acidic environments that degrade most sorbents, new sorbent materials are highly desirable. Here, efficient removal of Cs^+ and Sr^{2+} is achieved by the composite of layered tin sulfide $(Me_2NH_2)_{4/3}(Me_3NH)_{2/3}Sn_3S_7{\cdot}1.25H_2O$ (FJSM-SnS) and polyacrylonitrile (PAN) (FJSM-SnS/PAN). The granulous composite possesses regular particle morphology and good mechanical strength as an engineered form. It shows excellent acid−base and γ-irradiation resistance, high maximum adsorption capacities (q_m) of 296.12 and 62.88 mg/g for Cs^+ and Sr^{2+} ions, respectively, and high selectivity even in the presence of excess Na^+ ions or using lake water. Impressively, q_m^{Cs} of FJSM-SnS/PAN reaches 89.29 mg/g under even acidic conditions (pH = 2.5). The column loaded with FJSM-SnS/PAN granules exhibits high removal rates (R) toward low-concentration Cs^+ and Sr^{2+} ions under both neutral and acidic conditions. Moreover, the composite can be recycled and reused with high R^{Cs} and R^{Sr}. This work highlights the great potential of metal sulfide ion-exchangers in engineered form for the efficient removal of Cs^+ or Sr^{2+} ions, especially under acidic conditions, for radionuclide remediation.

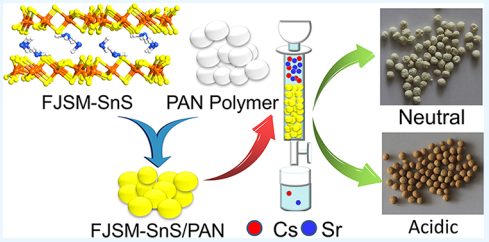

KEYWORDS: *Cesium, Strontium, Radionuclide remediation, Nuclear waste management, Layered metal sulfide, Polyacrylonitrile, Composite material*

INTRODUCTION

The continued development of nuclear energy is necessary given the high energy density and no emission of greenhouse gases it can afford. The nuclear waste disposal is one of the key problems for the development of nuclear energy.[1,2] ^{137}Cs ($t_{1/2}$ = 30.17 years) and ^{90}Sr ($t_{1/2}$ = 28.80 years) as relatively long half-life radionuclides are produced with high fission yields (6.18% for ^{137}Cs and 5.89% for ^{90}Sr) by nuclear fission of ^{235}U and/or ^{239}Pu after absorbing neutrons in a nuclear reactor.[3] They are considered highly hazardous because of the high-energy β- and γ-radiations. In particular, the highly soluble and mobile ionic forms of ^{137}Cs and ^{90}Sr with strong biological toxicity pose long-term threats to environmental safety and human health.[4−9] For instance, during the Fukushima incident ^{137}Cs and ^{90}Sr rapidly spread into the sea, causing considerable concern.[10] Although it is critical to remove ^{137}Cs and ^{90}Sr from nuclear waste, it is a great challenge to effectively and selectively do so because of the chemically complex aqueous solutions.[11−13] In particular, it is difficult to effectively remove Cs^+ and Sr^{2+} ions from acidic environments because of the effects of protonation of the ion-exchange materials and retardation of their performance.[14,15]

The commonly used methods for the removal of ^{137}Cs and ^{90}Sr include evaporation, precipitation, solvent extraction, biological treatment, adsorption, ion exchange, and so forth.[4,16−21] The ion exchange method holds great promise due to its low-cost, convenient operation, good selectivity, less solidified waste, and high efficiency.[22,23] Compared with organic ion exchangers,[24] inorganic ion exchangers usually show better chemical and thermal stability, irradiation resistance, and higher adsorption capacity or selectivity for Cs^+ and Sr^{2+} ions.[25−27] To date, various inorganic ion exchangers have been investigated, such as zeolites,[28,29] heteropoly acid salts,[30] ferrous metal cyanide compounds,[31,32] and titanium silicates.[33−35] Nevertheless, current ion-exchange materials usually suffer from low capacity, instabilities in acidic solutions, and poor selectivity. Metal sulfides are newly emerging Cs^+/Sr^{2+} ion exchangers showing high adsorption capacity and faster kinetic response, which is ascribed to their flexible frameworks and strong affinity of the soft Lewis basic sites of S^{2-} for moderately soft Lewis acids of Cs^+/Sr^{2+}.[6,36−45]

Ion-exchange columns are often necessary to achieve simple operation and low operating cost and are important for

Received: January 29, 2021
Accepted: March 1, 2021
Published: March 11, 2021

https://dx.doi.org/10.1021/acsami.1c01983
ACS Appl. Mater. Interfaces 2021, 13, 13434−13442

radioactive waste treatment.[46] The aforementioned very promising metal sulfide ion-exchangers generally are small particle-sized materials and columns made from them can block very easily with increasing back pressure.[45,47] Therefore, various engineered forms of metal sulfide ion-exchange materials should be developed for practical applications. To this end, forming composite material with regular particle morphology is attractive as it may improve the mechanical strength and solvent stability of materials.[45] To date, however, there are only a few examples of metal sulfide-based composites for ion removal, including KMS-1/PAN (KMS-1, $K_{2x}Mn_xSn_{3-x}S_6$, x = 0.5−0.95; PAN. polyacrylonitrile),[47] KMS-1/r-GO (r-GO: reduced graphene oxide),[48] PAN-chalcogel,[49] and KMS-2/CA (KMS-2: $K_{2x}Mg_xSn_{3-x}S_6$, x = 0.5−1; CA. calcium alginate).[50,51] Among them, KMS-1/PAN[47] and KMS-1/r-GO[48] were studied for the removal of Cs^+ or Sr^{2+} ions through batch experiments, whereas PAN-chalcogel[49] and KMS-2/CA[50,51] were loaded in a column to investigate removal of I^- ions and heavy metal ions such as Pb^{2+}, respectively. However, the removal of Cs^+ or Sr^{2+} ions using metal sulfide composites in an ion-exchange column has not been reported.

Polyacrylonitrile (PAN) with a series of advantages such as good pellet-forming ability, adhesion to inorganic materials, good thermal mechanical stability wear resistance and high tensile performance should be an ideal polymer matrix for preparing metal sulfide composites.[46,49,52−59] Herein, we describe a new composite adsorbent FJSM-SnS/PAN comprising layered tin sulfide $(Me_2NH_2)_{4/3}(Me_3NH)_{2/3}Sn_3S_7 \cdot 1.25H_2O$ (FJSM-SnS)[43,60] and PAN by a facile method that presents excellent acid−base and γ-irradiation resistance. Batch adsorption experiments show that FJSM-SnS/PAN retains high adsorption capacities and excellent selectivity for Cs^+ and Sr^{2+} ions in the presence of excessive Na^+ ions or under even tap and lake water. Particularly, the efficient removal of Cs^+ can be achieved by FJSM-SnS/PAN with q_m^{Cs} of 89.29 mg/g under even acidic conditions (pH = 2.5). Moreover, granulous FJSM-SnS/PAN composite possesses regular particle morphology and good mechanical strength as an engineered form. The ion-exchange column loaded with FJSM-SnS/PAN granules maintains high removal rates (R) toward low-concentration Cs^+ and Sr^{2+} ions under neutral and acidic conditions (pH = 2.5). The multiple elution-reuse experiments confirm the recyclability of FJSM-SnS/PAN. This work highlights the promise of metal-sulfide/PAN composites in radionuclide remediation field under a broad range of pH conditions.

EXPERIMENTAL SECTION

Synthesis of FJSM-SnS. FJSM-SnS was synthesized through the solvothermal method by heating a mixture of $SnCl_4 \cdot 5H_2O$, elemental sulfur, dimethylamine solution, and water at 180 °C for 7 days, as we previously reported.[43]

Synthesis of FJSM-SnS/PAN. FJSM-SnS/PAN composite microspheres were prepared by the following process. First, 1.00 g of FJSM-SnS powder sample was added to 6.00 mL of dimethyl sulfoxide (DMSO) under rapid stirring. PAN (0.40 g) was added to the above suspension and then the mixture was heated at 40 °C until a viscous suspension was formed. Then, the suspension was dropped into a beaker with large amount of water using a pipet. Granules were formed in the water, which were collected, further washed with water, and dried 10 h in an oven at 50 °C. When the drying temperature exceeded 80 °C, the composite would dissolve in the drying process; when the dosage of PAN was below 15%, the regular particle morphology of composite would not form. Finally, yellow granules of FJSM-SnS/PAN composite were obtained.

Batch Adsorption Experiments. Considering the high radioactivity of ^{137}Cs and ^{90}Sr, their nonradioactive isotopes were used as surrogates for batch adsorption experiments. All batch adsorption experiments were carried out at room temperature (RT), and the V (solution volume)/m (adsorbent weight) was 1000 mL/g. All of the ACl solutions (A = Cs^+, Sr^{2+}, K^+, Na^+) solutions used in the adsorption experiments were prepared from corresponding chlorides. The pH values of solutions were adjusted by adding NaOH and HCl solutions.

A typical batch adsorption experiment was performed as follows. A certain amount of crushed FJSM-SnS/PAN sample was added to a CsCl or $SrCl_2$ solution with the initial Cs^+ concentration (C_0^{Cs}) of 3000 mg/L or initial Sr^{2+} concentration (C_0^{Sr}) of 800 mg/L. The resulting mixture was stirred for 10 h at RT. Then the solid products were separated by centrifugation and filtration (denoted as FJSM-SnS/PAN-Cs and FJSM-SnS/PAN-Sr, respectively), which then were used for characterization analyses including powder X-ray diffraction patterns (PXRD), energy-dispersive spectroscopy (EDS), and X-ray photoelectron spectroscopy (XPS). The concentration of metal ion in the filtered solution was determined by inductively coupled plasma-mass spectroscopy (ICP-MS), inductively coupled plasma-optical emission spectroscopy (ICP-OES), or atomic absorption spectroscopy (AAS). All solution samples (including the standard and blank solution) were diluted with HNO_3 solution (2%) for the concentration test. More detailed information can be found in Supporting Information.

Ion-Exchange Column Experiments. The adsorption experiments under dynamic conditions, that is, ion-exchange column experiments, were studied under both neutral (pH = 7.1) and acidic (pH = 2.5) conditions. In a typical experiment, a sample of about 1.30 g of FJSM-SnS/PAN granules was packed into a glass tube column with an internal diameter of 13.40 mm, resulting in a height of about 2.00 cm. To avoid the loss of material, a small amount of cotton wool was placed at the bottom of the column. The Cs^+ and Sr^{2+} mixed solutions with the initial concentrations in the range of 0.94−1.00 mg/L for C_0^{Cs} and 0.99−1.10 mg/L for C_0^{Sr} were prepared. About 50 bed volumes of the above solution (140 mL) slowly passed through the column in 5 h, which was collected at the bottom into a 200 mL serum bottle. Finally, in this section 500−600 bed volume solutions (1.40−1.68 L) were tested. The concentration of the solutions after the column was analyzed using ICP-MS.

The Elution and Reusability Experiments. FJSM-SnS/PAN composites after ion exchange experiments were eluted with high-concentration KCl solution (0.30 M). About 1.00 g of sample was added to 50 mL of 0.30 M KCl solution which was slowly stirred under magnetic agitation at RT for 12 h. Finally, the sample (denoted as FJSM-SnS/PAN-elution) was further washed with water and dried in an oven at 80 °C overnight and then analyzed by EDS and PXRD. In the reusability assessment experiments, ∼0.70−1.20 g FJSM-SnS/PAN-elution granules were packed into a glass column with an internal diameter of 13.40 mm. The procedure was the same as the column experiments with pH = 7.1.

RESULTS AND DISCUSSION

Characterizations of FJSM-SnS/PAN, FJSM-SnS/PAN-Cs, and FJSM-SnS/PAN-Sr. The FJSM-SnS/PAN composite was obtained as yellow granules with a diameter of 2−3 mm as measured by Vernier calipers (Figure 1a,b). Scanning electron microscopy (SEM) images of PAN, FJSM-SnS, and FJSM-SnS/PAN indicate that FJSM-SnS/PAN retains the layered FJSM-SnS (Figure S1). PXRD patterns of FJSM-SnS, PAN and FJSM-SnS/PAN are shown in Figure 1c. The characteristic Bragg peaks corresponding to FJSM-SnS are present in the PXRD pattern of FJSM-SnS/PAN, and the additional peak at 10−17° is attributed to PAN. No extra reflections were observed in the PXRD pattern of FJSM-SnS/PAN, indicating

https://dx.doi.org/10.1021/acsami.1c01983
ACS Appl. Mater. Interfaces 2021, 13, 13434−13442

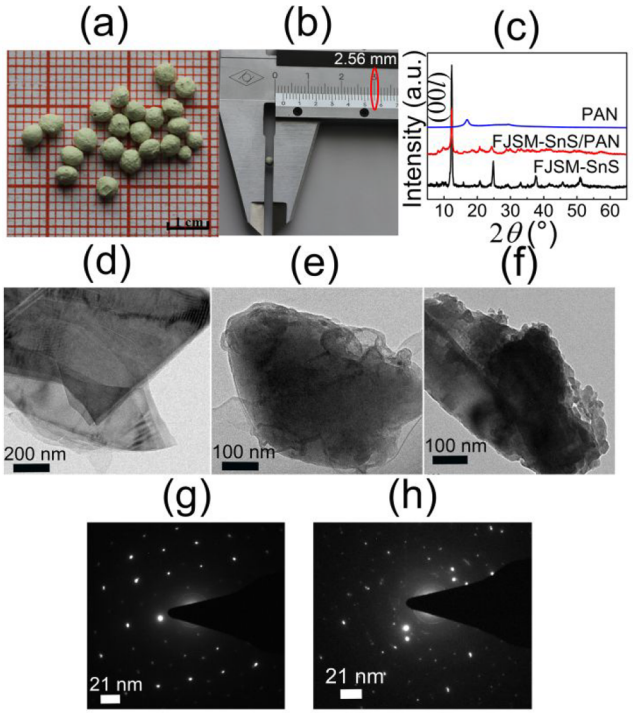

Figure 1. (a) Photograph of the granulous FJSM-SnS/PAN composite; (b) typical size of FJSM-SnS/PAN (2.56 mm) measured by a Vernier caliper (the specification is 0.02 mm); (c) PXRD patterns for pristine FJSM-SnS, PAN, and FJSM-SnS/PAN; TEM images of FJSM-SnS/PAN (d), FJSM-SnS/PAN-Cs (e), and FJSM-SnS/PAN-Sr (f); electron diffraction patterns of FJSM-SnS/PAN-Cs (g) and FJSM-SnS/PAN-Sr (h).

that FJSM-SnS and PAN successfully combined without changing the phase of FJSM-SnS and PAN.

The microscopic morphologies of FJSM-SnS/PAN-Cs and FJSM-SnS/PAN-Sr were consistent with that of pristine FJSM-SnS/PAN, as shown in the transmission electron microscopy (TEM) images (Figure 1d–f) and the electron diffraction patterns (Figure 1g,h). This confirms that the crystal lattice is retained after Cs^+ and Sr^{2+} adsorption, consistent with an ion exchange process. Compared with that of pristine FJSM-SnS/PAN, PXRD patterns of FJSM-SnS/PAN-Cs and FJSM-SnS/PAN-Sr show shifts of (00*l*) Bragg peaks to higher 2θ (lower *d*-spacing) indicating the expected decrease of the interlayer distance after the Cs^+ or Sr^{2+} ion-exchange (Figure S2). EDS analyses of the products after ion-exchange show the presence of Cs^+ or Sr^{2+} (Figure S3). The elemental distribution mapping confirms that Cs^+ or Sr^{2+} ions are uniformly distributed in the samples (Figure 2). XPS shows characteristic peaks of Cs (3d) for FJSM-SnS/PAN-Cs and Sr (3d) for FJSM-SnS/PAN-Sr, which further confirms the EDS results (Figure S4).

Adsorption Kinetics. Cs^+ or Sr^{2+} adsorption kinetics were studied under different contact time at pH of 7.1. The removal rate (*R*, eq S2) of FJSM-SnS/PAN for Cs^+ ions reaches 55.26% within 10 min and approaches 77.25% within 90 min, corresponding to a decrease of Cs^+ concentration from 9.32 to 2.12 mg/L (Figure 3a). The FJSM-SnS/PAN removed 60.64% Sr^{2+} ions within 15 min and captured 89.30% Sr^{2+} ions within 90 min, corresponding to a decrease of Sr^{2+} concentration from 9.35 to 1.00 mg/L (Figure 3b). Compared with the commercial UOP IONSIV I-911 (t_e^{Cs} > 4 h; t_e^{Sr} > 4 h),[61] the current composite shows more rapid adsorption kinetics at pH of 7.1. The kinetic data for Cs^+ and Sr^{2+} ions can be fitted with the pseudo-first-order kinetics model (eq S3) and the pseudo-second-order kinetics model (eq S4). The latter fit is better giving higher correlation coefficients (R^2 = 0.99981 for Cs^+ and 0.99982 for Sr^{2+}, Figure S5 and Table S2), indicating that the adsorption process is chemical sorption.[62−64]

Adsorption Isotherm Studies. To assess the maximum uptake capacities (q_m) of FJSM-SnS/PAN for Cs^+ and Sr^{2+} ions, the adsorption isotherm experiments were measured at pH = 7.1. The equilibrium adsorption data for Cs^+ and Sr^{2+} ions are fitted with both the Langmuir isotherm model (eq S5) and Freundlich isotherm model (eq S6). The Langmuir isotherm model describes the adsorption process of monolayer on a homogeneous surface of adsorbent with an identical number of binding sites.[65] The Freundlich isotherm model is an empirical model that possesses no saturated adsorption value, which takes into account multilayer adsorption that occurs on a heterogeneous surfaces with an undetermined active binding site.[66] In the Langmuir and Freundlich models, all adsorption sites are assumed to be equivalent, and only one ion can be captured at each site.[67−70] The adsorption behaviors of Cs^+ or Sr^{2+} for FJSM-SnS/PAN fit the Langmuir adsorption model with the high correlation coefficients R^2 (Figure 3c,d and Table S7). Accordingly, q_m^{Cs} and q_m^{Sr} are 296.12 and 62.88 mg/g, respectively.

As shown in Figure 3e and Table S14, the q_m^{Cs} for FJSM-SnS/PAN is higher than commercial sorbents under neutral conditions, such as ammonium molybdophosphate-polyacrylonitrile (AMP-PAN) (81.31 mg/g)[54] and hydrous crystalline sodium silicotitanate (TAM-5) (191.8 mg/g),[71] and exceeds other Cs^+ adsorption composite materials based on PAN, such as sodium titanosilicate-polyacrylonitrile (STS-PAN) (58.48 mg/g),[58] hydrous manganese oxide-polyacrylonitrile (HMO-PAN) (73.21 mg/g),[56] polyacrylonitrile-zeolite nanocomposite (PZNC) (214.1 mg/g),[53] polyacrylonitrile-potassium nickel

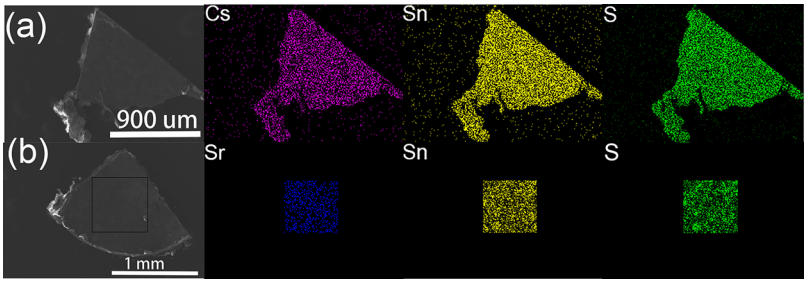

Figure 2. (a) SEM image and elemental distribution maps of Sn, S, and Cs for FJSM-SnS/PAN-Cs. (b) SEM image and elemental distribution maps of Sn, S, and Sr for FJSM-SnS/PAN-Sr.

https://dx.doi.org/10.1021/acsami.1c01983
ACS Appl. Mater. Interfaces 2021, 13, 13434−13442

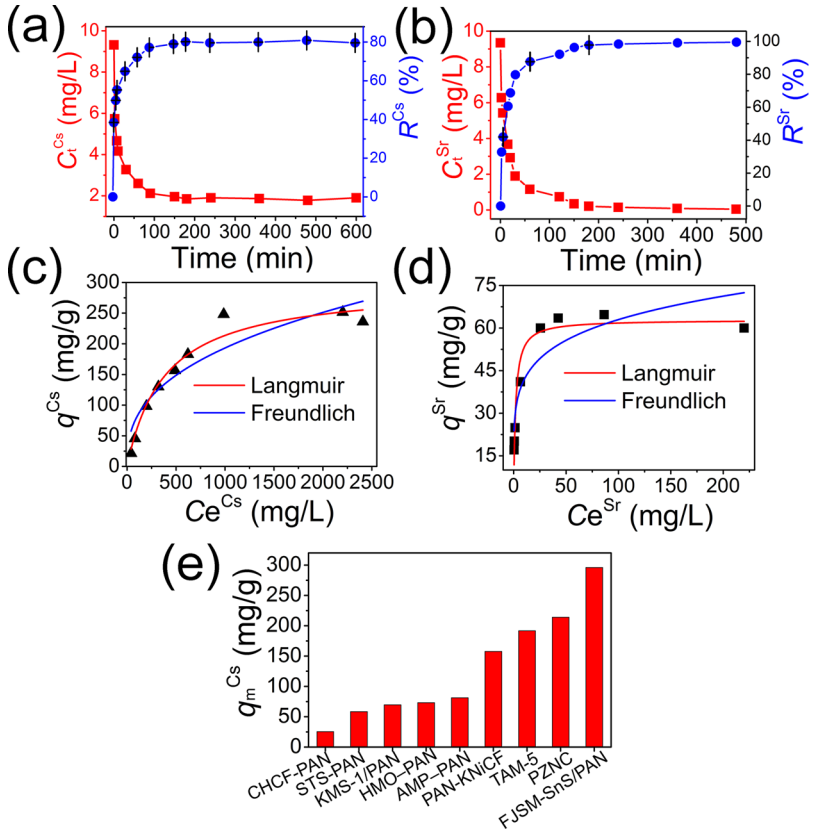

Figure 3. (a) Kinetics of FJSM-SnS/PAN for the removal of Cs^+ ions; (b) kinetics for Sr^{2+} ions plotted as a function of concentrations (mg/g) (red line) and their removal rate (%) (blue line) versus the time t (min), respectively (C_0^{Cs} = 9.32 ± 0.3 mg/L and contact time = 10 h, C_0^{Sr} = 9.35 mg/L, contact time = 8 h; V/m = 1000 mL/g; ~RT, pH = 7.1); equilibrium data for Cs^+ (c) and Sr^{2+} (d) ions adsorptions of FJSM-S/PANfitted with the Langmuir and Freundlich isotherm models (C_0^{Cs} in the range of 41.10−2408 mg/L and C_0^{Sr} in the range of 17.50−280 mg/L; V/m = 1000 mL/g, contact time = 10 h; ~RT, pH = 7.1); (e) the comparison of q_m^{Cs} values of FJSM-SnS/PAN with other reported sorbents.

hexacyanoferrates (PAN-KNiCF) (157.73 mg/g),[57] copper hexacyanoferrate-polyacrylonitrile (CHCF-PAN) (25.52 mg/g),[55] and the layered sulfide KMS-1/PAN (69.75 mg/g).[47] Although the values of q_m^{Cs} and q_m^{Sr} for FJSM-SnS/PAN decrease compared to FJSM-SnS itself (q_m^{Cs} = 408.91 mg/g, q_m^{Sr} = 65.15 mg/g at 65 °C), the composite possesses regular and large particle morphology and better mechanical strength and is more suitable as a practical engineered form. The lower q_m of Sr^{2+} for FJSM-SnS/PAN may be due to the larger volume of $[Sr(H_2O)_6]^{2+}$.[40] Similar phenomena have been observed in other sulfide ion exchangers such as pristine FJSM-SnS,[43] KMS-1,[40] and KMS-2.[6]

Effect of pH on Adsorption of Cs^+ or Sr^{2+} Ions. Previous studies have shown that FJSM-SnS has excellent acid/base resistance in the pH range of 0.6−12.[43,60] To further test the Cs^+ and Sr^{2+} removal abilities of the FJSM-SnS/PAN composite under acidic or basic conditions, we investigated the broad pH range of 0−11.4. The composite was soaked in acidic solutions with various concentrations of Cs^+ or Sr^{2+} ions for 10 h, after which the dissolution percentages of Sn were tested. The dissolution percentages of Sn reach 11.10% and 13.33% at pH = 0, respectively, whereas they both are 0.28% at pH = 0.4 (Table S4). Our previous studies also indicated that the dissolution percentages of Sn for FJSM-SnS varied from 0.13% to 0.09% in the pH range of 0.6−3.6.[60] Impressively, the removal rate R values for FJSM-SnS/PAN retained high levels from 80.18% to 90.04% for Cs^+ ions in the pH range of 4.6−9.5 and from 85.94% to 99.92% for Sr^{2+} ions in the pH range of 3.3−10.2, respectively. Notably, it removed around 69.17% of Cs^+ even in an acidic environment (pH = 2.4). However, the R^{Cs} was only 15.63% at pH of 0.4 and 12.20% at pH of 1.6, respectively. The results indicate that the composite exhibited its best efficiency for Cs^+ adsorption in the pH range of 2.4−11.4 (Table S5). Therefore, we chose to study the Cs^+ adsorption performance of FJSM-SnS/PAN at the pH of 2.5.

The distribution coefficients (K_d, eq S7) for Cs^+ ions range from 1.35 × 10^3 mL/g to 9.04 × 10^3 mL/g in the pH range of 2.4−11.4, while the K_d values of Sr^{2+} ions range from 4.71 × 10^2 to 1.28 × 10^6 mL/g in the pH range of 2.4−10.2 (Figure 4a,b). In addition, PXRD patterns of samples after Cs^+/Sr^{2+} ions adsorption in the pH range of 3.4−11.4 for Cs^+ ions and 3.4−10.2 for Sr^{2+} ions are in accord with that of pristine FJSM-SnS/PAN (Figure S6a,b), demonstrating the stability of FJSM-SnS/PAN composite during the adsorption experiments. At pH = 0.4 or 2.4, the PXRD patterns of Cs^+/Sr^{2+} ion adsorption products show the shift of the (00l) Bragg peak to higher 2θ, suggesting the ion exchange of the organic ammonium cations with H_3O^+ ions. This is similar to other layered ion exchange materials including pristine FJSM-SnS[60] and $Na_2Sn_3S_7$.[72]

The adsorption isotherm experiments of FJSM-SnS/PAN under acidic conditions were further performed. Consider that FJSM-SnS/PAN remains as the high R value of 69.17% for Cs^+ ions at pH = 2.4, which was much higher than R^{Cs} at pH = 0.4 or 1.6. The adsorption isotherm experiments were tested at pH = 2.5, and we observed that Cs^+ ions could be effectively removed at pH = 2.5 despite interference from H^+ ions. Figure

https://dx.doi.org/10.1021/acsami.1c01983
ACS Appl. Mater. Interfaces 2021, 13, 13434−13442

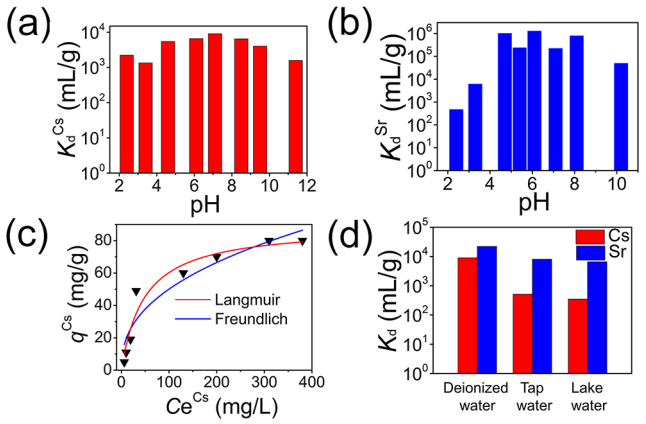

Figure 4. K_d values of Cs^+ (a) and Sr^{2+} (b) for FJSM-SnS/PAN at various initial pH values (C_0^{Cs} in the range of 4.52−7.98 mg/L, pH = 2.4−11.4; C_0^{Sr} in the range of 4.20−6.86 mg/L, pH = 2.4−10.2; V/m = 1000 mL/g, contact time = 10 h; ∼RT); (c) equilibrium data for Cs^+ ions adsorption for FJSM-SnS/PAN under acidic conditions fitted with the Langmuir and Freundlich isotherm models, (C_0^{Cs} in the range of 11−670 mg/L; V/m = 1000 mL/g, pH = 2.5; contact time: 10 h; RT); (d) K_d values of FJSM-SnS/PAN for Cs^+ or Sr^{2+} in various water environments (C_0^{Cs} in the range of 4.52−5.00 mg/L and C_0^{Sr} in the range of 5.60−6.50 mg/L; V/m = 1000 mL/g, contact time: 10 h; RT).

4c and Table S7 show that the Langmuir isotherm model describes well the adsorption behavior of Cs^+ (R^2 = 0.9449). The q_m^{Cs} of the FJSM-SnS/PAN sample reaches 89.29 mg/g at pH = 2.5.

To our knowledge, only a few adsorption studies of Cs^+ ions under acidic conditions have been reported, that is, SnSiMo (pH = 5, q_m = 16 mg/g),[73] HMO-PAN (pH = 5, q_m = 73.21 mg/g),[56] natural clinoptilolite (pH = 5, q_m = 49.02 mg/g),[74] magnetic Nb-substituted crystalline silicotitanate (Mag-Nb-CST) (pH = 4, q_m = 11.18 mg/g),[8] and NaFeTiO (pH = 4.1, q_m = 40.9 mg/g).[75] Compared with these adsorbents, the FJSM-SnS/PAN presents better acid resistance and higher adsorption capacity for Cs^+ under acidic conditions (Table S14).

Cs^+ and Sr^{2+} Separation in the Presence of Interfering Ions. Radioactive waste usually contains large amounts of diverse ions such as alkali or alkaline earth metal ions that can interfere with the separation process by competing for the sorbent. Among them, the high concentration of Na^+ ions poses a great challenge for the selective capture of target ions.[6,76] Hence, we investigated the Cs^+ and Sr^{2+} adsorption ability of FJSM-SnS/PAN in the presence of 0.88−757 mg/L Na^+ ions. The composite retained its high removal rates of Sr^{2+} ions in the presence of excess Na^+ ions. When the Na^+/Sr^{2+} mole ratios reach 1408.81 and 5622.18, it could still retain R^{Sr} of 90.27% and 81.85%, respectively (Figure S7a). Therefore, FJSM-SnS/PAN has excellent selectivity for Sr^{2+} ions. By contrast, the effect of massive excess Na^+ ions on Cs^+ ions was serious because of the competitive ion exchange. When the mole ratios of Na^+/Cs^+ ions varied from 4.26 to 3688.43, R^{Cs} values were 40.65% to 8.78% (Figure S7b). The very large excess of Na^+ ions in the solution partly saturate the Cs^+ ion adsorption sites of FJSM-SnS/PAN.

Adsorption in Tap Water and Lake Water. The abilities of FJSM-SnS/PAN for the Cs^+ or Sr^{2+} removal in various water environments, such as deionized water, tap water (Fuzhou city, Fujian 2018), and lake water (Fuzhou Xihu lake, September 2018) were investigated. We simulated deionized water, tap water, and lake water contaminated by Cs^+ or Sr^{2+} with the initial concentration of 4.52−5.00 mg/L for Cs^+ and 5.60−6.50 mg/L for Sr^{2+} ions, respectively. K_d^{Cs} and R^{Cs} values in tap water and lake water are 5.24 × 10^2 mL/g and 34.40%, and 3.51 × 10^2 mL/g and 26.00%, respectively, which is lower than that in deionized water (K_d^{Cs} = 9.04 × 10^3 mL/g and R^{Cs} = 90.04%) (Figure 4d and Table S9). Compared with K_d^{Sr} and R^{Sr} values in deionized water (K_d^{Sr}, 2.21 × 10^5 mL/g; R^{Sr}, 99.55%), K_d^{Sr} and R^{Sr} in tap water and lake water can still reach 8.06 × 10^3 mL/g and 88.96% and 6.63 × 10^3 mL/g and 86.89%, respectively. Therefore, FJSM-SnS/PAN can retain good selectivity for Sr^{2+} ions in these water environments.

Effects of Irradiation. It is necessary that the sorbent materials for radionuclide remediation possess excellent radiation resistance.[39,77] Therefore, we conducted a preliminary investigation of effects of γ-irradiation on Cs^+ and Sr^{2+} ions adsorption of FJSM-SnS/PAN. The detailed information about the irradiation experiments can be found in Supporting Information. The FJSM-SnS/PAN sample was irradiated under 100 kGy γ radiation for 178.57 h or 200 kGy γ radiation for 377.56 h, respectively. PXRD patterns of samples after γ-irradiation remain unchanged compared with the pristine, indicating the good irradiation resistance of FJSM-SnS/PAN (Figure 5a). In the solution of mixed Cs^+ and Sr^{2+} ions (C_0^{Cs},

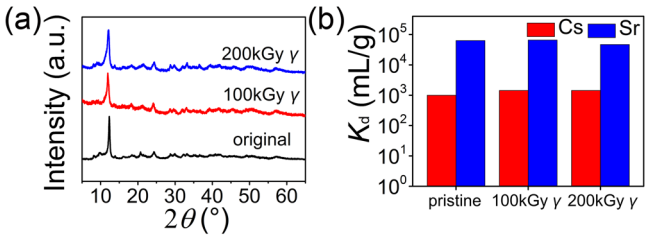

Figure 5. (a) PXRD patterns of the pristine, γ (100 and 200 kGy) irradiated samples of FJSM-SnS/PAN. (b) K_d values of Cs^+ and Sr^{2+} for γ-irradiated samples compared with those of pristine FJSM-SnS/PAN (C_0^{Cs} = 17.80 mg/L C_0^{Sr} = 16.70 mg/L; V/m = 1000 mL/g, contact time: 10 h; RT).

17.79 mg/L; C_0^{Sr}, 16.70 mg/L), the K_d values of the sample after 100 kGy γ irradiation were 1.44 × 10^3 mL/g for Cs^+ and 6.58 × 10^4 mL/g for Sr^{2+}. K_d^{Cs} and K_d^{Sr} of sample after 200 kGy γ-irradiation were 1.43 × 10^3 mL/g and 4.67 × 10^4 mL/g, respectively (Figure 5b and Table S10). Thus, the Cs^+ and Sr^{2+} removal capacities of FJSM-SnS/PAN were retained even after strong γ-irradiation, further indicating the irradiation resistance of FJSM-SnS/PAN and its potential for application in practical radioactive wastewater treatment.

Sorbent Recovery by Elution. The recovery and reusability of sorbent materials are important to evaluate their potential in practical use. Here, a high concentration KCl solution (0.3 M) was used to conduct elution experiments on the FJSM-SnS/PAN-Cs and FJSM-SnS/PAN-Sr under stirring at room temperature. The eluted samples are denoted as FJSM-SnS/PAN-Cs-K and FJSM-SnS/PAN-Sr-K, respectively. EDS analyses and the elemental distribution mappings also show that the Cs^+ and Sr^{2+} ions were completely removed and replaced by K^+ ions which were evenly distributed in the samples (Figures S8 and S9). PXRD patterns of FJSM-SnS/

https://dx.doi.org/10.1021/acsami.1c01983
ACS Appl. Mater. Interfaces 2021, 13, 13434−13442

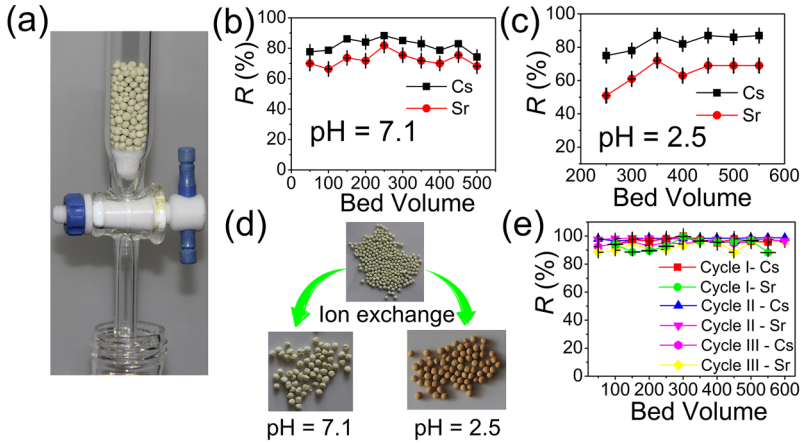

Figure 6. (a) An ion-exchange column made with the granulous FJSM-SnS/PAN composite; (b) removal rates for Cs^+ and Sr^{2+} by FJSM-SnS/PAN in an ion-exchange column experiment at pH = 7.1 plotted against bed volume; (c) removal rates for Cs^+ and Sr^{2+} at pH = 2.5 plotted against bed volume; (d) granulous FJSM-SnS/PAN composite samples before and after ion-exchange column experiments under pH = 7.1 or pH = 2.5 conditions; (e) removal rates of Cs^+ and Sr^{2+} by FJSM-SnS/PAN-elution samples in multiple-cycle experiments.

PAN-Cs-K show that the pristine layered framework of FJSM-SnS in the composite remained unchanged (Figure S10).

Ion-Exchange Column Studies. Continuous bed flow ion-exchange column operations are commonly used in many industrial wastewater treatment processes. However, if the size of the adsorbent is very small, there is instability against particle flow. As a result, high packing of particles and column blocking phenomena occur which hinder further practical application. The granulous FJSM-SnS/PAN composite with a diameter of about 2 mm was then loaded in a column of an internal diameter of 13.40 mm and a height of about 2.00 cm to perform the ion-exchange experiments (Figure 6a). Mixed solutions (pH = 7.1) containing Cs^+ and Sr^{2+} passed through slowly (0.5 mL/min) the column. The composite in column experiments exhibited high removal rate for low concentration Cs^+ and Sr^{2+} ions (C_0^{Cs}, 0.94−0.97 mg/L; C_0^{Sr}, 1.07−1.10 mg/L) within 500 bed volumes (Table S11). After processing 250 bed volumes of the mixture solution (700 mL), R^{Cs} and R^{Sr} reached 88.29% and 82.10%, respectively. After processing 450 bed volumes of the mixture solution (1.26 L), R^{Cs} and R^{Sr} could still reach 82.75% and 75.59%, respectively (Figure 6b).

We then further studied the ion-exchange column of FJSM-SnS/PAN under acidic conditions (pH = 2.5). The FJSM-SnS/PAN column exhibited high removal rates for low-concentration Cs^+ and Sr^{2+} ions (C_0^{Cs} and C_0^{Sr} in the range of 0.99−1.00 mg/L) within 550 bed volumes under pH of 2.5 (Table S12). After processing 450 bed volumes (1.26 L), R^{Cs} and R^{Sr} could still reach 86.61% and 68.85%, respectively (Figure 6c). Compared with R^{Cs} and R^{Sr} under neutral conditions, the abilities of the ion-exchange column to remove low-concentration Cs^+ and Sr^{2+} ions under acidic solutions remained. After the treatment of Cs^+ and Sr^{2+} ions under the neutral and acid conditions, the composite granules still retained their shape, confirming the excellent mechanical strength of FJSM-SnS/PAN (Figure 6d). After processing the acidic solutions by the ion-exchange column, the color of FJSM-SnS/PAN granules became darker (signifying protonation of S^{2-} to SH) while it retained its regular shape (Figure 6d). This confirms the good mechanical strength of the granules under acidic conditions.

Since the FJSM-SnS/PAN granules in the ion-exchange column after elution (FJSM-SnS/PAN-elution) maintain their shape (Figure S11), we performed back-ion-exchange (using K ions rather than dimethylammonium or trimethylammonium ions) to regenerate the sorbent for use in a subsequent cycle of Cs^+ and Sr^{2+} removal experiments. Compared with the pristine FJSM-SnS/PAN, the regenerated FJSM-SnS/PAN-elution granules in the ion-exchange column after processing 500 bed volumes exhibited comparable removal abilities for the Cs^+ and Sr^{2+} ions to the original pristine composite (e.g., 73.51% to 96.12% for R^{Cs} versus 68.59% to 96.72% for R^{Sr}). Therefore, the K^+ ions play the same role in moving in and out of the layered sulfide structure as the original methylammonium ions. After three cycles of elution-reuse experiments, R^{Cs} and R^{Sr} of the composite granules could still reach 96.43% and 96.33%, respectively (Tables S13, Figure 6e).

CONCLUSION

The granulous FJSM-SnS/PAN composite has excellent γ-irradiation resistance and acid−base resistance (pH = 2.4−11.4), good regeneration ability, and high adsorption capacities (q_m^{Cs}, 296.12 mg/g and q_m^{Sr}, 62.88 mg/g at pH = 7.1; q_m^{Cs}, 89.29 mg/g at pH = 2.5) and high selectivity (K_d^{Cs}, 9.04×10^3 mL/g; K_d^{Sr}, 1.28×10^6 mL/g) for Cs^+ and Sr^{2+} ions. The ion-exchange column loaded with FJSM-SnS/PAN granules shows excellent removal performance for low-concentration Cs^+ and Sr^{2+} ions even under acidic conditions with removal rates of 86.61% and 68.85% for Cs^+ and Sr^{2+}, respectively, at pH = 2.5. Moreover, owing to the regular particle morphology and good mechanical strength, FJSM-SnS/PAN granules can be recycled in the application of ion-exchange column, maintaining high removal rates of 96.43% for Cs^+ and 96.33% for Sr^{2+} even after multiple cycles of elution-reuse. These results reveal the potential of FJSM-SnS/PAN composite as an attractive engineered form of sorbent for radioactive wastewater management.

ASSOCIATED CONTENT

Supporting Information

The Supporting Information is available free of charge at https://pubs.acs.org/doi/10.1021/acsami.1c01983.

Experimental section, PXRD, EDS, XPS, mapping, and equations and tables for ion-exchange data (PDF)

https://dx.doi.org/10.1021/acsami.1c01983
ACS Appl. Mater. Interfaces 2021, 13, 13434−13442

AUTHOR INFORMATION

Corresponding Authors

Meiling Feng − *State Key Laboratory of Structural Chemistry, Fujian Institute of Research on the Structure of Matter, Chinese Academy of Sciences, Fuzhou, Fujian 350002, P.R. China; Department of Chemistry, Northwestern University, Evanston, Illinois 60208, United States; University of Chinese Academy of Sciences, Beijing 100049, P.R. China;* orcid.org/0000-0003-2524-0994; Email: fml@fjirsm.ac.cn

Mercouri G. Kanatzidis − *Department of Chemistry, Northwestern University, Evanston, Illinois 60208, United States;* orcid.org/0000-0003-2037-4168; Email: m-kanatzidis@northwestern.edu

Authors

Jilong Li − *State Key Laboratory of Structural Chemistry, Fujian Institute of Research on the Structure of Matter, Chinese Academy of Sciences, Fuzhou, Fujian 350002, P.R. China; College of Chemistry and Materials Science, Fujian Normal University, Fuzhou, Fujian 350007, P.R. China*

Jiance Jin − *State Key Laboratory of Structural Chemistry, Fujian Institute of Research on the Structure of Matter, Chinese Academy of Sciences, Fuzhou, Fujian 350002, P.R. China; University of Chinese Academy of Sciences, Beijing 100049, P.R. China;* orcid.org/0000-0002-4876-2018

Yanmin Zou − *State Key Laboratory of Structural Chemistry, Fujian Institute of Research on the Structure of Matter, Chinese Academy of Sciences, Fuzhou, Fujian 350002, P.R. China*

Haiyan Sun − *State Key Laboratory of Structural Chemistry, Fujian Institute of Research on the Structure of Matter, Chinese Academy of Sciences, Fuzhou, Fujian 350002, P.R. China; University of Chinese Academy of Sciences, Beijing 100049, P.R. China*

Xi Zeng − *State Key Laboratory of Structural Chemistry, Fujian Institute of Research on the Structure of Matter, Chinese Academy of Sciences, Fuzhou, Fujian 350002, P.R. China; University of Chinese Academy of Sciences, Beijing 100049, P.R. China*

Xiaoying Huang − *State Key Laboratory of Structural Chemistry, Fujian Institute of Research on the Structure of Matter, Chinese Academy of Sciences, Fuzhou, Fujian 350002, P.R. China; University of Chinese Academy of Sciences, Beijing 100049, P.R. China;* orcid.org/0000-0002-3514-216X

Complete contact information is available at: https://pubs.acs.org/10.1021/acsami.1c01983

Author Contributions

J.L., M.F., and M.G.K. conceived the project. J.L. and M.F. designed and carried out all of the experiments. Y.Z., H.S., and X.Z. offered help in the theoretical knowledge, experiment, and software operating. J.L. prepared the first draft of the manuscript. J.J., M.F., X.H., and M.G.K. revised the manuscript. All of the authors discussed the results and commented on the manuscript. M.F. and M.G.K. supervised the project.

Notes

The authors declare no competing financial interest.

ACKNOWLEDGMENTS

The authors gratefully acknowledge the financial support provided by the National Science Foundations of China (Grants 22076185 and 21771183), NSF of Fujian Province (Grant 2020J06033), the FJIRSM&IUE Joint Research Fund (Grant RHZX-2018-005) (m.M.F.). At Northwestern University the work was supported in part by the National Science Foundation through grant DMR-2003476 (M.G.K.).

REFERENCES

(1) Khanal, L. R.; Sundararajan, J. A.; Qiang, Y. Advanced Nanomaterials for Nuclear Energy and Nanotechnology. *Energy Technol.* **2020**, *8* (3), 1901070.

(2) Tian, G. X.; Wang, J. C.; Shen, Y. F.; Rao, L. F. Extraction of Strontium from HLLW Using N,N,N',N'-Tetraisobutyl 3-Oxaglutaramide. *Solvent Extr. Ion Exch.* **2005**, *23* (4), 519−528.

(3) Emara, A. M.; El-Sweify, F. H.; Abo-Zahra, S. F.; Hashim, A. I.; Siyam, T. E. Removal of Cs-137 and Sr-90 from Reactor Actual Liquid Waste Samples Using a New Synthesized Bionanocomposite-based Carboxymethylcellulose. *Radiochim. Acta* **2019**, *107* (8), 695−711.

(4) Lauchnor, E. G.; Schultz, L. N.; Bugni, S.; Mitchell, A. C.; Cunningham, A. B.; Gerlach, R. Bacterially Induced Calcium Carbonate Precipitation and Strontium Coprecipitation in a Porous Media Flow System. *Environ. Sci. Technol.* **2013**, *47* (3), 1557−1564.

(5) Vincent, T.; Vincent, C.; Barre, Y.; Guari, Y.; Le Saout, G.; Guibal, E. Immobilization of Metal Hexacyanoferrates in Chitin Beads for Cesium Sorption: Synthesis and Characterization. *J. Mater. Chem. A* **2014**, *2* (26), 10007−10021.

(6) Mertz, J. L.; Fard, Z. H.; Malliakas, C. D.; Manos, M. J.; Kanatzidis, M. G. Selective Removal of Cs^{+}, Sr^{2+}, and Ni^{2+} by $K_{2x}Mg_xSn_{3-x}S_6$ (x = 0.5−1) (KMS-2) Relevant to Nuclear Waste Remediation. *Chem. Mater.* **2013**, *25* (10), 2116−2127.

(7) Romanovskiy, V. N.; Smirnov, I. V.; Babain, V. A.; Todd, T. A.; Herbst, R. S.; Law, J. D.; Brewer, K. N. The Universal Solvent Extraction (UNEX) Process. I. Development of The UNEX Process Solvent for the Separation of Cesium, Strontium, and the Actinides from Acidic Radioactive Waste. *Solvent Extr. Ion Exch.* **2001**, *19* (1), 1−21.

(8) Zhao, X. D.; Meng, Q. H.; Chen, G.; Wu, Z. H.; Sun, G. G.; Yu, G. B.; Sheng, L. S.; Weng, H. Q.; Lin, M. Z. An Acid-resistant Magnetic Nb-substituted Crystalline Silicotitanate for Selective Separation of Strontium and/or Cesium Ions From Aqueous Solution. *Chem. Eng. J.* **2018**, *352*, 133−142.

(9) Ivanov, Y. A.; Lewyckyj, N.; Levchuk, S. E.; Prister, B. S.; Firsakova, S. K.; Arkhipov, N. P.; Arkhipov, A. N.; Kruglov, S. V.; Alexakhin, R. M.; Sandalls, J.; Askbrant, S. Migration of ^{137}Cs and ^{90}Sr from Chernobyl fallout in Ukrainian, Belarussian and Russian Soils. *J. Environ. Radioact.* **1997**, *35* (1), 1−21.

(10) Chino, M.; Nakayama, H.; Nagai, H.; Terada, H.; Katata, G.; Yamazawa, H. Preliminary Estimation of Release Amounts of ^{131}I and ^{137}Cs Accidentally Discharged from the Fukushima Daiichi Nuclear Power Plant into the Atmosphere. *J. Nucl. Sci. Technol.* **2011**, *48* (7), 1129−1134.

(11) Ghandhi, S. A.; Weber, W.; Melo, D.; Doyle-Eisele, M.; Chowdhury, M.; Guilmette, R.; Amundson, S. A. Effect of ^{90}Sr Internal Emitter on Gene Expression in Mouse Blood. *BMC Genomics* **2015**, *16*, 586.

(12) Robertson, H. A.; Falconer, I. R. Accumulation of Radioactive Iodine in Thyroid Glands Subsequent to Nuclear Weapon Tests and the Accident at Windscale. *Nature* **1959**, *184* (4700), 1699−1702.

(13) Wang, J. L.; Zhuang, S. T. Removal of Cesium Ions from Aqueous Solutions Using Various Separation Technologies. *Rev. Environ. Sci. Bio/Technol.* **2019**, *18* (2), 231−269.

(14) Xiao, C.; Fard, Z. H.; Sarma, D.; Song, T. B.; Xu, C.; Kanatzidis, M. G. Highly Efficient Separation of Trivalent Minor Actinides by a Layered Metal Sulfide ($KInSn_2S_6$) from Acidic Radioactive Waste. *J. Am. Chem. Soc.* **2017**, *139* (46), 16494−16497.

(15) Zhang, X.; Gu, P.; Liu, Y. Decontamination of Radioactive Wastewater: State of the Art and Challenges Forward. *Chemosphere* **2019**, *215*, 543−553.
(16) Villard, A.; Siboulet, B.; Toquer, G.; Merceille, A.; Grandjean, A.; Dufreche, J.-F. Strontium Selectivity in Sodium Nonatitanate $Na_4Ti_9O_{20}\cdot xH_2O$. *J. Hazard. Mater.* **2015**, *283*, 432−438.
(17) Kumar, P.; Pournara, A.; Kim, K. H.; Bansal, V.; Rapti, S.; Manos, M. J. Metal-organic Frameworks: Challenges and Opportunities for Ion-exchange/sorption Applications. *Prog. Mater. Sci.* **2017**, *86*, 25−74.
(18) Liu, X.; Pang, H.; Liu, X.; Li, Q.; Zhang, N.; Mao, L.; Qiu, M.; Hu, B.; Yang, H.; Wang, X. Orderly Porous Covalent Organic Frameworks-based Materials: Superior Adsorbents for Pollutants Removal from Aqueous Solutions. *Innovation* **2021**, *2* (1), 100076.
(19) Wang, J. L.; Zhuang, S. T. Cesium Separation from Radioactive Waste by Extraction and Adsorption Based on Crown Ethers and Calixarenes. *Nucl. Eng. Technol.* **2020**, *52* (2), 328−336.
(20) Wang, J. L.; Chen, C. Biosorbents for Heavy Metals Removal and Their Future. *Biotechnol. Adv.* **2009**, *27* (2), 195−226.
(21) Chen, Y.; Wang, J. Removal of Radionuclide Sr^{2+} Ions from Aqueous Solution Using Synthesized Magnetic Chitosan Beads. *Nucl. Eng. Des.* **2012**, *242*, 445−451.
(22) Rahman, R. O. A.; Ibrahium, H. A.; Hung, Y. T. Liquid Radioactive Wastes Treatment: A Review. *Water* **2011**, *3* (2), 551−565.
(23) Lehto, J.; Harjula, R. Selective Separation of Radionuclides from Nuclear Waste Solutions with Inorganic Ion Exchangers. *Radiochim. Acta* **1999**, *86* (1−2), 65−70.
(24) Hassan, N. M.; McCabe, D. J.; King, W. D.; Hamm, L. L.; Johnson, M. E. Ion Exchange Removal of Cesium from Hanford Tank Waste Supernates SuperLig (R) 644 Resin. *J. Radioanal. Nucl. Chem.* **2002**, *254* (1), 33−40.
(25) Clearfield, A. Inorganic Ion Exchangers, Past, Present, and Future. *Solvent Extr. Ion Exch.* **2000**, *18* (4), 655−678.
(26) Figueiredo, B. R.; Cardoso, S. P.; Portugal, I.; Rocha, J.; Silva, C. M. Inorganic Ion Exchangers for Cesium Removal from Radioactive Wastewater. *Sep. Purif. Rev.* **2018**, *47* (4), 306−336.
(27) Trgo, M.; Peric, J.; Medvidovic, N. V. A Comparative Study of Ion Exchange Kinetics in Zinc/lead-modified Zeolite-clinoptilolite Systems. *J. Hazard. Mater.* **2006**, *136* (3), 938−945.
(28) Abusafa, A.; Yucel, H. Removal of ^{137}Cs from Aqueous Solutions Using Different Cationic Forms of a Natural Zeolite: Clinoptilolite. *Sep. Purif. Technol.* **2002**, *28* (2), 103−116.
(29) Dyer, A.; Chimedtsogzol, A.; Campbell, L.; Williams, C. Uptake of Caesium and Strontium Radioisotopes by Natural Zeolites from Mongolia. *Microporous Mesoporous Mater.* **2006**, *95* (1−3), 172−175.
(30) El-Khouly, S. H. Separation of Europium, Cobalt and Zinc on Zirconium Tungstate Ion Exchanger. *J. Radioanal. Nucl. Chem.* **2006**, *270* (2), 391−398.
(31) Valsala, T. P.; Roy, S. C.; Shah, J. G.; Gabriel, J.; Raj, K.; Venugopal, V. Removal of Radioactive Caesium from Lowlevel Radioactivewaste (LLW) Streams Using Cobalt Ferrocyanide Impregnated Organic Anion Exchanger. *J. Hazard. Mater.* **2009**, *166* (2−3), 1148−1153.
(32) Wang, J. L.; Zhuang, S. T.; Liu, Y. Metal Hexacyanoferrates-based Adsorbents for Cesium Removal. *Coord. Chem. Rev.* **2018**, *374*, 430−438.
(33) Solbra, S.; Allison, N.; Waite, S.; Mikhalovsky, S. V.; Bortun, A. I.; Bortun, L. N.; Clearfield, A. Cesium and Strontium Ion Exchange on the Framework Titanium Silicate $M_2Ti_2O_3SiO_4\cdot nH_2O$ (M = H, Na). *Environ. Sci. Technol.* **2001**, *35* (3), 626−629.
(34) Celestian, A. J.; Clearfield, A. The Origin of Ion Exchange Selectivity in A Porous Framework Titanium Silicate. *J. Mater. Chem.* **2007**, *17* (46), 4839−4842.
(35) Celestian, A. J.; Kubicki, J. D.; Hanson, J.; Clearfield, A.; Parise, J. B. The Mechanism Responsible for Extraordinary Cs Ion Selectivity in Crystalline Silicotitanate. *J. Am. Chem. Soc.* **2008**, *130* (35), 11689−11694.
(36) Manos, M. J.; Kanatzidis, M. G. Highly Efficient and Rapid Cs^+ Uptake by the Layered Metal Sulfide $K_{2x}Mn_xSn_{3-x}S_6$ (KMS-1). *J. Am. Chem. Soc.* **2009**, *131* (18), 6599−6607.
(37) Ding, N.; Kanatzidis, M. G. Selective Incarceration of Caesium Ions by Venus Flytrap Action of a Flexible Framework Sulfide. *Nat. Chem.* **2010**, *2* (3), 187−191.
(38) Feng, M. L.; Kong, D. N.; Xie, Z. L.; Huang, X. Y. Three-dimensional Chiral Microporous Germanium Antimony Sulfide with Ion-exchange Properties. *Angew. Chem., Int. Ed.* **2008**, *47* (45), 8623−8626.
(39) Yang, H.; Luo, M.; Luo, L.; Wang, H.; Hu, D.; Lin, J.; Wang, X.; Wang, Y.; Wang, S.; Bu, X.; Feng, P.; Wu, T. Highly Selective and Rapid Uptake of Radionuclide Cesium Based on Robust Zeolitic Chalcogenide Via Stepwise Ion-exchange Strategy. *Chem. Mater.* **2016**, *28* (23), 8774−8780.
(40) Manos, M. J.; Ding, N.; Kanatzidis, M. G. Layered Metal Sulfides: Exceptionally Selective Agents for Radioactive Strontium Removal. *Proc. Natl. Acad. Sci. U. S. A.* **2008**, *105* (10), 3696−3699.
(41) Sarma, D.; Malliakas, C. D.; Subrahmanyam, K. S.; Islama, S. M.; Kanatzidis, M. G. $K_{2x}Sn_{4-x}S_{8-x}$ (x = 0.65−1): a New Metal Sulfide for Rapid and Selective Removal of Cs^+, Sr^{2+} and UO_2^{2+} Ions. *Chem. Sci.* **2016**, *7* (2), 1121−1132.
(42) Wang, K. Y.; Ding, D.; Sun, M.; Cheng, L.; Wang, C. Effective and Rapid Adsorption of Sr^{2+} Ions by a Hydrated Pentasodium Cluster Templated Zinc Thiostannate. *Inorg. Chem.* **2019**, *58* (15), 10184−10193.
(43) Qi, X. H.; Du, K. Z.; Feng, M. L.; Li, J. R.; Du, C. F.; Zhang, B.; Huang, X. Y. A Two-dimensionally Microporous Thiostannate with Superior Cs^+ and Sr^{2+} Ion-exchange Property. *J. Mater. Chem. A* **2015**, *3* (10), 5665−5673.
(44) Feng, M. L.; Sarma, D.; Gao, Y. J.; Qi, X. H.; Li, W. A.; Huang, X. Y.; Kanatzidis, M. G. Efficient Removal of $[UO_2]^{2+}$, Cs^+, and Sr^{2+} Ions by Radiation-resistant Gallium Thioantimonates. *J. Am. Chem. Soc.* **2018**, *140* (35), 11133−11140.
(45) Manos, M. J.; Kanatzidis, M. G. Metal Sulfide Ion Exchangers: Superior Sorbents for Capture of Toxic and Nuclear Waste-related Metal Ions. *Chem. Sci.* **2016**, *7* (8), 4804−4824.
(46) Tranter, T. J.; Herbst, R. S.; Todd, T. A.; Olson, A. L.; Eldredge, H. B. Evaluation of Ammonium Molybdophosphate-polyacrylonitrile (AMP-PAN) as a Cesium Selective Sorbent for The Removal of ^{137}Cs from Acidic Nuclear Waste Solutions. *Adv. Environ. Res.* **2002**, *6* (2), 107−121.
(47) Wang, Y. X.; Li, J. R.; Yang, J. C. E.; Yuan, B. L.; Fu, M. L. Granulous KMS-1/PAN Composite for Cs^+ Removal. *RSC Adv.* **2015**, *5* (111), 91431−91435.
(48) Gupta, K.; Yuan, B. L.; Chen, C.; Varnakavi, N.; Fu, M. L. $K_{2x}Mn_xSn_{3-x}S_6$ (x = 0.5−0.95) (KMS-1) Immobilized on the Reduced Graphene Oxide as KMS-1/r-GO Aerogel to Effectively Remove Cs^+ and Sr^{2+} from Aqueous Solution. *Chem. Eng. J.* **2019**, *369*, 803−812.
(49) Riley, B. J.; Pierce, D. A.; Chun, J.; Matyas, J.; Lepry, W. C.; Garn, T. G.; Law, J. D.; Kanatzidis, M. G. Polyacrylonitrile-chalcogel Hybrid Sorbents for Radioiodine Capture. *Environ. Sci. Technol.* **2014**, *48* (10), 5832−5839.
(50) Rapti, S.; Pournara, A.; Sarma, D.; Papadas, I. T.; Armatas, G. S.; Tsipis, A. C.; Lazarides, T.; Kanatzidis, M. G.; Manos, M. J. Selective Capture of Hexavalent Chromium from an Anion-exchange Column of Metal Organic Resin-alginic Acid Composite. *Chem. Sci.* **2016**, *7* (3), 2427−2436.
(51) Kanatzidis, M. G.; Sarma, D.; Manos, E. Ion-exchange Column Used to Remove Metal Ions from Sample Comprising Metal Ions, Comprises Column and Ion-exchange Material Comprising Composite Material that Comprises Metal Chalcogenide and Alginate, and Inert Granular Material. US 2015144568-A1; WO 2015080976-A1; CA 2927398-A1; AU 2014354984-A1; EP 3074128-A1; JP 2017500189-W; EP 3074128-A4; AU 2014354984-B2; JP 6517799-B2; US 10549270-B2.
(52) Nilchi, A.; Khanchi, A.; Atashi, H.; Bagheri, A.; Nematollahi, L. The Application and Properties of Composite Sorbents of Inorganic

https://dx.doi.org/10.1021/acsami.1c01983
ACS Appl. Mater. Interfaces 2021, 13, 13434−13442

Ion Exchangers and Polyacrylonitrile Binding Matrix. *J. Hazard. Mater.* **2006**, *137* (3), 1271−1276.
(53) Faghihian, H.; Iravani, M.; Moayed, M.; Ghannadi-Maragheh, M. A Novel Polyacrylonitrile-zeolite Nanocomposite to Clean Cs and Sr from Radioactive Waste. *Environ. Chem. Lett.* **2013**, *11* (3), 277−282.
(54) Park, Y.; Lee, Y. C.; Shin, W. S.; Choi, S. J. Removal of Cobalt, Strontium and Cesium from Radioactive Laundry Wastewater by Ammonium Molybdophosphate-polyacrylonitrile (AMP-PAN). *Chem. Eng. J.* **2010**, *162* (2), 685−695.
(55) Nilchi, A.; Saberi, R.; Moradi, M.; Azizpour, H.; Zarghami, R. Adsorption of Cesium on Copper Hexacyanoferrate-PAN Composite Ion Exchanger from Aqueous Solution. *Chem. Eng. J.* **2011**, *172* (1), 572−580.
(56) Oh, S.; Shin, W. S.; Choi, S. J. Hydrous Manganese Oxide-polyacrylonitrile (HMO-PAN) Composite for the Treatment of Radioactive Laundry Wastewater. *J. Radioanal. Nucl. Chem.* **2015**, *303* (1), 495−508.
(57) Du, Z. H.; Jia, M. C.; Wang, X. W. Cesium Removal from Solution Using PAN-based Potassium Nickel Hexacyanoferrate(II) Composite Spheres. *J. Radioanal. Nucl. Chem.* **2013**, *298* (1), 167−177.
(58) Saberi, R.; Nilchi, A.; Garmarodi, S. R.; Zarghami, R. Adsorption Characteristic of ^{137}Cs from Aqueous Solution Using PAN-based Sodium Titanosilicate Composite. *J. Radioanal. Nucl. Chem.* **2010**, *284* (2), 461−469.
(59) Nilchi, A.; Saberi, R.; Garmarodi, S. R.; Bagheri, A. Evaluation of PAN-based Manganese Dioxide Composite for the Sorptive Removal of Cesium-137 from Aqueous Solutions. *Appl. Radiat. Isot.* **2012**, *70* (2), 369−374.
(60) Gao, Y. J.; Sun, H. Y.; Li, J. L.; Qi, X. H.; Du, K. Z.; Liao, Y. Y.; Huang, X. Y.; Feng, M. L.; Kanatzidis, M. G. Selective Capture of Ba^{2+}, Ni^{2+}, and Co^{2+} by a Robust Layered Metal Sulfide. *Chem. Mater.* **2020**, *32* (5), 1957−1963.
(61) Huckman, M. E.; Latheef, I. M.; Anthony, R. G. Ion Exchange of Several Radionuclides on the Hydrous Crystalline Silicotitanate, UOP IONSIV IE-911. *Sep. Sci. Technol.* **1999**, *34* (6−7), 1145−1166.
(62) Ho, Y. S. Review of Second-order Models for Adsorption Systems. *J. Hazard. Mater.* **2006**, *136* (3), 681−689.
(63) Wang, J. L.; Guo, X. Adsorption Kinetic Models: Physical Meanings, Applications, and Solving Methods. *J. Hazard. Mater.* **2020**, *390*, 122156.
(64) Guo, X.; Wang, J. L. A General Kinetic Model for Adsorption: Theoretical Analysis and Modeling. *J. Mol. Liq.* **2019**, *288*, 111100.
(65) Langmuir, I. The Adsorption of Gases on Plane Surfaces of Glass, Mica and Platinum. *J. Am. Chem. Soc.* **1918**, *40*, 1361−1403.
(66) Freundlich, H. Über Die Adsorption in Lösungen. *Z. Phys. Chem.* **1907**, *57U* (1), 385−470.
(67) El-Kamash, A. M. Evaluation of Zeolite A for the Sorptive Removal of Cs^{+} and Sr^{2+} Ions from Aqueous Solutions Using Batch and Fixed Bed Column Operations. *J. Hazard. Mater.* **2008**, *151* (2−3), 432−445.
(68) Abdel-Ghani, N. T.; Rawash, E. S. A.; El-Chaghaby, G. A. Equilibrium and Kinetic Study for the Adsorption of *P*-nitrophenol from Wastewater Using Olive Cake Based Activated Carbon. *Global J. Environ. Sci. Manage.* **2016**, *2* (1), 11−18.
(69) Wang, J.; Guo, X. Adsorption Isotherm Models: Classification, Physical Meaning, Application and Solving Method. *Chemosphere* **2020**, *258*, 127279.
(70) Guo, X.; Wang, J. L. Comparison of Linearization Methods for Modeling the Langmuir Adsorption Isotherm. *J. Mol. Liq.* **2019**, *296*, 111850.
(71) Zheng, Z.; Philip, C. V.; Anthony, R. G.; Krumhansl, J. L.; Trudell, D. E.; Miller, J. E. Ion Exchange of Group I Metals by Hydrous Crystalline Silicotitanates. *Ind. Eng. Chem. Res.* **1996**, *35* (11), 4246−4256.
(72) Zhang, Z.; Gu, P.; Zhang, M.; Yan, S.; Dong, L.; Zhang, G. Synthesis of a Robust Layered Metal Sulfide for Rapid and Effective Removal of Sr^{2+} from Aqueous Solutions. *Chem. Eng. J.* **2019**, *372*, 1205−1215.
(73) Abdel-Galil, E. A.; Hassan, R. S.; Eid, M. A. Assessment of Nano-sized Stannic Silicomolybdate for the Removal of ^{137}Cs, ^{90}Sr, and ^{141}Ce Radionuclides from Radioactive Waste Solutions. *Appl. Radiat. Isot.* **2019**, *148*, 91−101.
(74) Smičiklas, I.; Dimović, S.; Plećaš, I. Removal of Cs^{+}, Sr^{2+} and Co^{2+} from Aqueous Solutions by Adsorption on Natural Clinoptilolite. *Appl. Clay Sci.* **2007**, *35* (1−2), 139−144.
(75) Amesh, P.; Suneesh, A. S.; Venkatesan, K. A.; Maheswari, R. U.; Vijayalakshmi, S. Preparation and Ion Exchange Studies of Cesium and Strontium on Sodium Irontitanate. *Sep. Purif. Technol.* **2020**, *238*, 116393.
(76) Zhang, P. C.; Wang, L.; Du, K.; Wang, S. Y.; Huang, Z. W.; Yuan, L. Y.; Li, Z. J.; Wang, H. Q.; Zheng, L. R.; Chai, Z. F.; Shi, W. Q. Effective Removal of U(VI) and Eu(III) by Carboxyl Functionalized MXene Nanosheets. *J. Hazard. Mater.* **2020**, *396*, 122731.
(77) Zhang, J. R.; Chen, L. H.; Dai, X.; Zhu, L.; Xiao, C. L.; Xu, L.; Zhang, Z. Y.; Alekseev, E. V.; Wang, Y. X.; Zhang, C.; Zhang, H. W.; Wang, Y. L.; Diwu, J.; Chai, Z. F.; Wang, S. Distinctive Two-step Intercalation of Sr^{2+} into a Coordination Polymer with Record High ^{90}Sr Uptake Capabilities. *Chem.* **2019**, *5* (4), 977−994.

https://dx.doi.org/10.1021/acsami.1c01983
ACS Appl. Mater. Interfaces 2021, 13, 13434−13442